



Computational Analysis of Current and Noise Properties of a Single Open Ion Channel

Enrico Piccinini,[†] Fabio Affinito,[‡] Rossella Brunetti,^{*,‡} Carlo Jacoboni,[‡] and Massimo Rudan[†]

Advanced Research Center on Electronic Systems and Dipartimento di Ingegneria Elettronica, Informatica e Sistemistica, Alma Mater Studiorum, Università di Bologna, Bologna, Italy, and Consiglio Nazionale delle Ricerche—Istituto Nazionale di Fisica della Materia S3 Research Center and Dipartimento di Fisica, Università di Modena e Reggio Emilia, Modena, Italy

Received June 21, 2006

Abstract: This paper presents a computational analysis of the noise associated with the ion current in single open ion channels. The study is performed by means of a coupled molecular dynamics/Monte Carlo approach able to simulate the conduction process on the basis of all microscopic information today available from protein structural data and atomistic simulations. The case of potassium ions permeating the KcsA channel is considered in the numerical calculations. The results show a noise spectrum different from what is theoretically predicted for Poisson noise, confirmed by the existence of a correlation in ion-exit events.

Introduction

Rather than merely a bothersome phenomenon, noise in biological systems is a useful property.¹ Before the patch-clamp technique was developed, current noise across biological membranes provided the first experimental evidence for the existence of ion-conducting pores with discrete conductance levels. Single-channel recording techniques are nowadays widely accessible, and open-channel noise can be measured with a standard experimental setup. However, noise analysis to study the kinetics of ions permeating a membrane channel is at present still a difficult task, because it is actually not possible to detect the individual shot events using the patch-clamp technique. The associated noise is so much faster than the time resolution of typical amplifiers used that it would not contribute much variance to the signal at the experimental filter settings;² however, it is possible to measure the increase in the white noise level when the channel opens.^{3,4}

From the computational side, the availability of X-ray crystallographic structures with atomic resolution⁵ provided

the necessary input to molecular dynamics (MD) analyses.⁶ MD provides atomistic information about the system and confirms that the permeation process takes place as a single-file concerted motion of ions. MD, however, is unable to provide directly the electrical properties of ionic flux due to the long time scale involved in the physiological permeation process. In the literature, a coupled MD–Brownian dynamics method has already been proposed⁷ to simulate conduction properties of potassium ions inside KcsA which reproduces the experimental data only at low applied voltages (also referred to in the following as “low-bias range”). From the computational point of view, in a Brownian dynamics trajectory, only few events resulting in the hopping of ions can be observed, and such translocations normally occur a few times per nanosecond: most of the simulation time is spent for intrasite thermal motion. Alternatively, the analysis of conduction properties through an analytical solution of a kinetic model has recently been reported.⁸

The aim of this work is to study the conduction and noise properties of potassium ions in the KcsA channels by means of a coupled molecular dynamics/Monte Carlo (MD/MC) simulation that yields both the current and its noise for a single channel under open-gate conditions and overcomes the numerical problems discussed above. The MC approach presented in this paper provides a numerical solution of the

* Corresponding author tel.: +39 059 205 5277; fax: +39 059 205 5616; e-mail: brunetti.rossella@unimore.it.

[†] Università di Bologna.

[‡] Università di Modena e Reggio Emilia.

kinetic equation and allows the exploration of a more detailed and accurate microscopic model. Furthermore, the simulation can be “biased” in order to enhance the sampling of rare events.

As in the methods available in the literature, a multi-ion model based on the existence of ion binding sites inside the protein and at the protein boundaries is the starting point of the framework. The MD/MC procedure can be summarized in the following steps:

1. Select relevant states for the channel’s binding-site occupation during the permeation process, and classify them into categories on the basis of translocation homology.

2. Run atomistic classical MD simulations without any applied external electric field, and obtain free-energy profiles for the previously identified transitions.

3. Determine rates for transitions between minima on the basis of a kinetic model. The same rate is associated with all of the transitions belonging to the same category, but differences may exist within the same category, depending on the direction of the flux.

4. Alter transition rates through the introduction of the effect of the external electric field assuming stepwise potential drops.

5. Perform MC simulations with the obtained rates to get the ion current as a numerical solution to this kinetic model.

6. Analyze ion-current fluctuations using tools from the noise analysis.

Partial results obtained from the MD/MC simulation of the ion permeation process include evaluations of the relevant energy barriers along given transition paths on the free-energy profile (end of step 2), current–voltage characteristics comparable with experiments⁹ (end of step 5), and noise power spectra for different transmembrane potentials (end of step 6).

The analysis of open-channel current fluctuations confirms that the motions of the ions in the selectivity filter are strongly correlated, and a quantitative estimate of the degree of correlation between consecutive ion exits from the channel can be evaluated.

Theoretical Basis

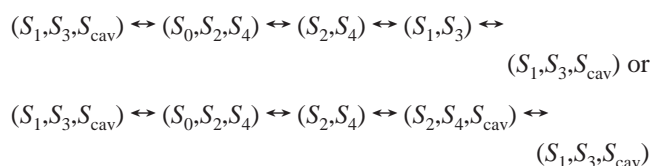
(a) Conduction Model. It has been established from structural^{5,10} and computational¹¹ analyses that the KcsA channel exhibits six stable binding sites, usually referred to as S_0 through S_4 and S_{cav} , in which, alternatively, potassium ions and water molecules reside. Furthermore, because of the strong electrostatic repulsion between ions inside the filter, ion hopping inside the channel takes place as a synchronous concerted motion of many ions, each ion moving from one site to an adjacent one. A free-energy barrier exists between two given ion occupancy configurations. These barriers range from few $k_B T$ ’s to many tens of $k_B T$ ’s (k_B is the Boltzmann constant and T the temperature in Kelvin), which suggests that only a restricted set of transitions actually determines the conduction properties of the channel.

The identification of the relevant configurations must account for a number of constraints imposed by what we know today from the atomic knowledge of the channel

protein. The configurations used in the simulation of the permeation process presented in this paper have been selected taking into account the following constraints:⁷ (a) single-file ion motion; (b) transitions involving configurations where ions moving inside the selectivity filter are allowed only through concerted motion; (c) fewer than two ions in the selectivity filter (sites S_1 – S_4) are not accepted to prevent an unstable conformation of the selectivity filter itself.

As previously reported,⁷ for an ion flux toward the extracellular environment, conduction is driven by the motion of ions from the cavity to site S_4 and, subsequently, by the concerted motion of ions in S_3 and S_1 into sites S_2 and S_0 . In the following, we describe with greater detail the translocation path of a single ion from the intracellular reservoir to the extracellular environment (and vice versa).

The four-step cycles



are composed of a three-ion concerted motion [later indicated with the label (t)], a two-ion concerted motion [label (d)], an entry/exit in the cavity site S_{cav} [label (c)], and an exit/entry in the outer mouth site S_0 [label (m)], as already adopted.⁸ Generally speaking, all of the possible transitions resulting from the reported rules can be classified into the aforementioned four groups, on the basis of how many ions simultaneously move, the occupation of the cavity site, or the outer mouth site. We also point out that the three-ion motion described above does not conflict with the translocation picture reported in the literature.⁷ As a matter of fact, once the potassium ion in the cavity enters site S_4 , previously filled with a water molecule, it forces this latter to the intermediate position between sites S_3 and S_4 .¹² Because of both steric constraints and electrical repulsion between adjacent potassium ions, this configuration immediately either turns back into its original one or evolves to (S_0, S_2, S_4) . The lifetime of the intermediate state is so short that this state may be ignored in the simulation for conduction purposes.

All of the transition rates can, in principle, be obtained, in the absence of an external field, by MD simulations as averages over many occurrences of the same pathway in the configuration space. In practice, each transition event requires MD simulation times too long to be spontaneously observed, and techniques designed in order to map specific regions of the free-energy profile (typically, umbrella sampling,¹³ steered MD,^{14,15} and metadynamics¹⁶) must be applied to circumvent this difficulty. The accuracy of the above-mentioned numerical estimates is dependent on the choice of the selected force field and reaction coordinates, and the numerical techniques used to speed up computational convergence. A comparison among results obtained from the three techniques on a test case based on an internal ion translocation within the KcsA protein is discussed elsewhere.¹⁷ The probability per unit time $k_{A \rightarrow B}$ to undergo a transition from channel configuration A to configuration B is then calculated using the transition-state theory:

$$k_{A \rightarrow B} = A \exp(-\beta \epsilon_b) \quad (1)$$

The prefactor A may be expressed by¹⁸ $A = \beta(M\omega_1\omega_2 D/2\pi)$, where D is the ion diffusion coefficient inside the channel, ϵ_b is the free-energy barrier separating the two states, M is the ion mass, ω_1 and ω_2 represent the parabolic-approximation parameters around the maximum and minimum of the energy profile as functions of the appropriate reaction coordinate, and $\beta = 1/k_B T$.

Equation 1, above, has been derived for a generic one-dimensional reaction coordinate. The representation of a multidimensional free-energy landscape, as the present case, strictly depends on the particular choice of the reaction coordinates, so that around minima and maxima paraboloids can be obtained with a different curvature for each chosen coordinate. Thus, the approximating frequencies depend on the curvilinear coordinate following the considered transition pathway and may vary from one representation to another. The order of magnitude of the parameters used in our simulations has been determined by a parabolic approximation of the maxima and minima in the one-dimensional free-energy profile as functions of the curvilinear coordinate; their final values have been fine-tuned applying detailed balance, so that in equilibrium conditions a net zero current results at zero bias.

The resulting transition rates used to generate the permeation paths in the MC procedure range from $1.08 \times 10^8 \text{ s}^{-1}$ to $9.93 \times 10^8 \text{ s}^{-1}$ and have been determined for a symmetric concentration of 100 mM of potassium ions in the reservoirs. A different concentration may affect both prefactors and barriers.

(b) Noise Analysis. Our noise analysis is restricted to the contribution coming from the electric current fluctuations generated by single-file diffusion through the very narrow channel in its open configuration. These current fluctuations are expected to arise from the discrete nature of current flow (ions move in discrete steps across the membrane) yielding “shot noise” analogous to what is observed in electronic devices. Additional sources of noise are associated with fluctuations of the energy barriers due to both thermal structural fluctuations of the protein and fluctuations on the protein structure coming from the interaction between the protein and the lipid bilayer. A third source of noise is associated with the gating process of the channel. The characteristic time scales of the three fluctuations listed above are different: nanoseconds for shot noise, picoseconds to nanoseconds for protein structural fluctuations (as MD simulations suggest), and milliseconds for fluctuations due to gating.⁹

Noise spectra in the frequency domain of the last two processes above have been experimentally obtained and studied in the past.^{3,19} The contribution to the total noise spectrum coming from shot noise associated with ion flow is still difficult to measure. It can be observed in the low-frequency range as an increase in the “white” noise background when the channel opens. In the high-frequency range, the main limit comes from the noise associated with electrodes and electronics. A theoretical analysis of ion current fluctuations in these nanometric biological conductors

on the nanosecond time scale is feasible only through the implementation of advanced atomistic approaches. This is actually the focus of our calculations. To this purpose, we assume that the channel is permanently in the open configuration. Furthermore, we will not consider the fluctuations in excess coming from internal motions of the channel protein. Theoretical calculations of current-noise spectra during single-file transport have been performed in the past by means of the analytical solution of macroscopic time-dependent single-file transport equations, based on a number of limiting hypotheses concerning the number of binding sites and ions inside the channel.²⁰ These calculations suggest that the presence of interactions between the ions in the channel can produce damped oscillations in the autocorrelation function of the microscopic current fluctuations. The availability of protein structural information and atomistic simulators allows us to calculate these noise properties on the basis of a more sound and general physical scheme and, in the future, to compare computational results with experimental results, now achievable with modern noise equipment. The autocorrelation function $C(\tau)$ of the current fluctuations $\delta I(t)$ can be numerically computed from the MC simulation assuming a stationary process. The spectral density of the current $S_I(\omega)$ is then obtained either by Fourier transforming $C(\tau)$ or by directly averaging the squared Fourier transform of the current fluctuations.

The classical theory of shot noise²¹ assumes that charge transport occurs by means of instantaneous processes and that the charge movements are totally uncorrelated in time. A parameter defined as the noise-to-signal ratio for a random variable n , which could be estimated from a time window that, on average, contains several random events, is the Fano factor F :²²

$$F = \frac{\sigma^2(n)}{\langle n \rangle} \quad (2)$$

where $\sigma^2(n)$ is the variance associated with the random variable and $\langle n \rangle$ is its mean value, both evaluated within the time step Δt . For the case here investigated, n is the number of ions crossing the channel mouth in the time interval Δt . Considering that ions flow across the channel in both directions, it holds that

$$n = n^+ - n^- \quad (3a)$$

where n^+ and n^- refer to the number of ions moving in the two opposite directions, and

$$\sigma^2(n) = \sigma^2(n^+ - n^-) = \sigma^2(n^+) + \sigma^2(n^-) - 2 \text{cov}(n^+, n^-) \quad (3b)$$

$\text{cov}(n^+, n^-)$ being the covariance of the two fluxes. By means of eqs 3a and 3b, eq 2 can be rewritten as

$$F = \frac{\sigma^2(n^+) + \sigma^2(n^-) - 2 \text{cov}(n^+, n^-)}{\langle n^+ \rangle - \langle n^- \rangle} \quad (4)$$

When the total current is determined by the sum of two independent, totally uncorrelated, opposite currents, the covariance term appearing in eq 3b vanishes and eq 4 reads

$$F^* = \frac{\sigma^2(n^+) + \sigma^2(n^-)}{\langle n^+ \rangle - \langle n^- \rangle} = \frac{\langle n^+ \rangle + \langle n^- \rangle}{\langle n^+ \rangle - \langle n^- \rangle} \quad (5)$$

Thus, the comparison between F and F^* gives information about the degree of correlation in the charge motion. Furthermore, it can be easily proved that

$$\lim_{\Delta t \rightarrow \infty} \frac{1}{\Delta t} \langle \delta Q_t^2 \rangle = \frac{1}{2} S_I(0) \quad (6)$$

where Q_t is the estimator of the total charge flowing across the channel mouth in the time interval Δt and $S_I(0)$ is the current noise power spectrum at zero frequency. We observe that $I = Q_t/\Delta t$ and $Q_t = n(t)q$, q being the charge of the moving particle and I being the current. Combining eq 2 with eq 6, one can obtain the well-known expression for the Fano factor:²¹

$$F = \frac{S_I(0)}{2q\langle I \rangle} \quad (7)$$

Methods

The simulated system is built by embedding the KcsA structure from *Streptomyces lividans* solved at 2.0 Å (PDB code 1K4C) in a water–octane–water bilayer.¹¹ The crystallographic structure has been obtained when the channel is in its closed state; we suppose here that the open-state structure does not modify significantly the selectivity filter region, which is under investigation in this study. For an analogous reason—a small influence of the membrane on the energy profile in the selectivity filter—we mimic the membrane environment with a simple octane slab and not with more sophisticated lipids in order to minimize the computational effort.

The system is thus composed of 420 amino acids, 500 octane molecules, 8802 water molecules (including crystallographic waters), 8 potassium ions, and 24 chlorine ions to ensure an electroneutral environment, for a total of 34 434 atoms.

The free-energy profiles have been determined via MD simulations using the GROMACS 3.3 package with the default GROMACS (or modified GROMOS87) force field^{23,24} in the NVT ensemble. Even though this force field is somewhat obsolete, it always proved to be satisfactory in correctly keeping the position of the binding sites after the equilibration time and was adopted because of this evidence. Several previous simulations with AMBER6 did not satisfy this preliminary test. Periodic boundary conditions have been applied to the simulation box ($69 \times 69 \times 97$ Å), and electrostatic interactions have been calculated with the particle mesh Ewald method.²⁵ The temperature has been kept constant with the Nosé–Hoover thermostat with a time constant of 5 fs; the Parrinello–Rahman barostat is used to control the pressure. Time steps of 1 fs have been applied.

The X-ray crystallographic structure has initially been fully equilibrated for 1.2 ns, in which the first 200 ps have been spent to increase the temperature from 100 to 300 K. Umbrella sampling free-energy calculations have been performed by applying a biasing harmonic potential (force constant used: 8368 kJ/mol nm²) to one of the ions involved

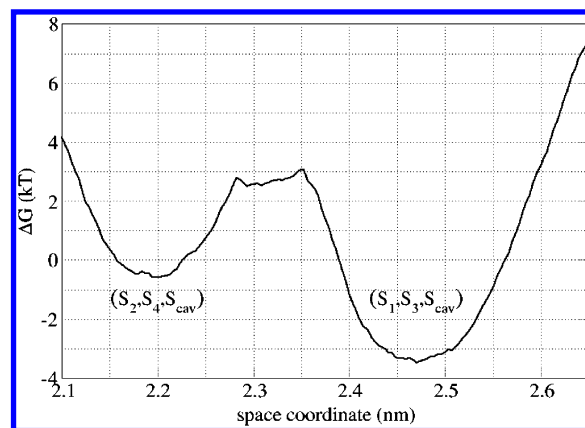


Figure 1. Free-energy profile as a function of the center of mass coordinate of the two top ions for transition $(S_2, S_4, S_{\text{cav}}) \rightarrow (S_1, S_3, S_{\text{cav}})$. The energy barrier is approximately $3.5 k_B T$ for the forward transition and $6.5 k_B T$ for the reverse transition.

in the conduction process. Because of the physical constraint of concerted motion inside the selectivity filter, this choice proved to be effective to induce the complete concerted translocation of all of the ions involved. The biasing potential was moved in steps of a half angstrom along the channel axis for a total of 18 space windows per trajectory. Each simulation lasted 500 ps, the first 300 ps being discarded as equilibration time in the presence of the added potential. The WHAM algorithm²⁶ was finally used to determine the free-energy profile.

An example of an equilibrium multi-ion free-energy profile is reported in Figure 1. The 1D curve represents the free energy as a function of the center of mass coordinate of the ions initially in the 2 and 4 binding sites for the transition $(S_2, S_4, S_{\text{cav}}) \leftrightarrow (S_1, S_3, S_{\text{cav}})$. The energy barrier obtained for this transition is approximately $3.5 k_B T$ for forward motion and $6.5 k_B T$ for backward motion, which is consistent with what is reported in the literature⁷ for two-ion concerted motion. Similar MD calculations have been performed to estimate the energy barriers affecting each class of translocations. Rates involving entries to or exits from the cavity site S_{cav} have been inferred from corresponding rates affecting analogous events in site S_0 , because under open-gate conditions the cavity is directly linked to the “inner bath”, as the outer mouth can freely communicate with its corresponding “outer bath”.

Finally, a few words must be spent on the 1D umbrella sampling, which may appear to be an oversimplified method to evaluate the free-energy profiles. In the past, calculations were performed using the positions of two or three ions in the selectivity filter as reaction coordinates;^{6,7} such calculations however are very demanding in terms of CPU time. From the analysis of the results available in the literature, one may note that in every single step of the conduction cycle only one coordinate varies significantly, the others being close to their initial values. This evidence suggests the possibility of implementing a 1D sampling of the free-energy profile. On the other hand, a good estimate of the ionic current and of the error affecting the energy barriers is of great importance for the appropriate evaluation of the free-

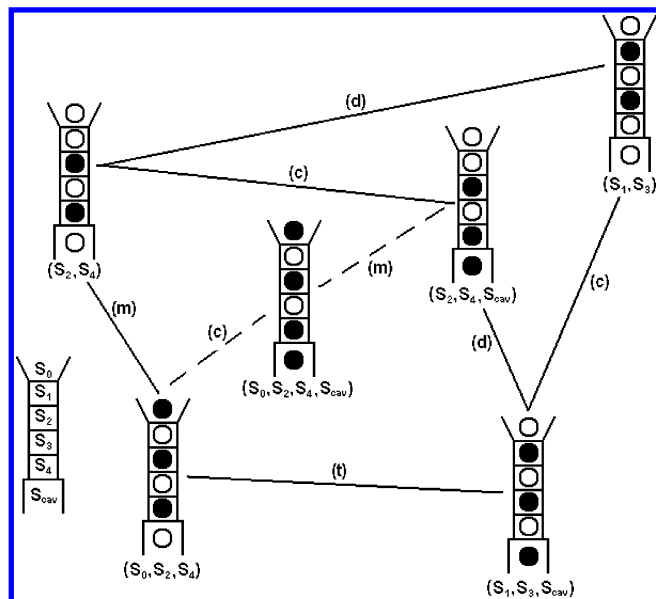


Figure 2. Configurations considered in the model and transitions among them. The sketch on the left is intended to show the six binding sites. Open circles stand for water molecules, solid circles for potassium ions. The dashed lines represent a transition with four ions involved that seldom happens. (m) stands for an ion entry/exit into/from the outer mouth S_0 , (c) for an exit/entry from/into the cavity site S_{cav} , (d) for the two-ion concerted motion, and (t) for the three-ion concerted motion. The set of transition rates at zero bias used in the MC simulations is the following: $(S_1, S_3) \rightarrow (S_2, S_4)$ and $(S_1, S_3, S_{cav}) \rightarrow (S_2, S_4, S_{cav})$: $1.08 \times 10^8 \text{ s}^{-1}$; $(S_2, S_4) \rightarrow (S_1, S_3)$ and $(S_2, S_4, S_{cav}) \rightarrow (S_1, S_3, S_{cav})$: $2.14 \times 10^8 \text{ s}^{-1}$; $(S_1, S_3) \rightarrow (S_1, S_3, S_{cav})$, $(S_2, S_4) \rightarrow (S_2, S_4, S_{cav})$, and $(S_0, S_2, S_4) \rightarrow (S_0, S_2, S_4, S_{cav})$: $9.93 \times 10^8 \text{ s}^{-1}$; $(S_1, S_3, S_{cav}) \rightarrow (S_1, S_3)$, $(S_2, S_4, S_{cav}) \rightarrow (S_2, S_4)$, and $(S_0, S_2, S_4, S_{cav}) \rightarrow (S_0, S_2, S_4)$: $2.07 \times 10^8 \text{ s}^{-1}$; $(S_2, S_4) \rightarrow (S_0, S_2, S_4)$ and $(S_2, S_4, S_{cav}) \rightarrow (S_0, S_2, S_4, S_{cav})$: $2.58 \times 10^8 \text{ s}^{-1}$; $(S_0, S_2, S_4) \rightarrow (S_2, S_4)$ and $(S_0, S_2, S_4, S_{cav}) \rightarrow (S_2, S_4, S_{cav})$: $1.73 \times 10^8 \text{ s}^{-1}$; $(S_0, S_2, S_4) \rightarrow (S_1, S_3, S_{cav})$: $8.61 \times 10^8 \text{ s}^{-1}$; $(S_1, S_3, S_{cav}) \rightarrow (S_0, S_2, S_4)$: $1.35 \times 10^8 \text{ s}^{-1}$.

energy profile. More results can be found in the literature¹⁷ and in a further work in preparation.

The conduction process is simulated by generating a sequence of transitions between different channel configurations through a Monte Carlo code. The available configurations and their transition rates at zero bias are reported in Figure 2.

The ion current has been evaluated as the net flux of incoming and outgoing charges at a channel boundary in a defined time interval Δt .

Power spectra have finally been calculated by Fourier transforming the current fluctuations $\delta I(t)$ and averaging results over 1000 independent sequences of 10 000 time steps.

To extract $I(V)$ characteristics starting from an atomistic approach, one must first deal with the problem of the effect of the external electric field on the transition rates. This has been done with the following constraint: after a complete cycle, the system (protein + ions inside) changes its total energy by an amount equal to qV , where V is the external

applied potential and q is the electronic charge that crossed the channel during the cycle.

Equation 1 now reads

$$k'_{A \rightarrow B} = A \exp[-\beta(\epsilon_b - q\alpha_b V)] = k_{A \rightarrow B} \exp(\beta q \alpha_b V) \quad (8)$$

to take into account the effect of the applied potential. Parameters α_b represent the fractions of the total potential applied to the transitions considered and will be further discussed in this section; the subscript b is a label classifying the kind of the considered transition.

The energetics of ion conduction in the presence of an electric field, to our knowledge, have not been deeply developed with a full self-consistent procedure so far. Even if technically possible,^{27,28} the presence of charged ions in the aqueous solution and the periodic boundary conditions make it difficult to implement an explicit electric field in the MD simulations. To overcome this problem, we choose to perform all of the MD simulations and the evaluation of the corresponding free-energy profiles without any external electric field. Only after calculating the transition rates at zero applied bias, we did consider the effect of the electric field by introducing a correcting factor, as reported in eq 8. To estimate how much a transition is affected by the applied external electric field, we referred to the milestone work of Bernèche and Roux,⁷ where the potential drop through the channel is calculated by means of a Poisson–Boltzmann scheme. It should be noted that this procedure applies rigorously only for the motion of a single ion at a time, that is, when all of the process can be described using one physical coordinate that also coincides with the reaction coordinate. On the contrary, when a multiplicity of coordinates must be taken into account, the procedure fails, and the potential drop should be further tuned to fit the experimental data, after its first evaluation via MD at zero bias. For the sake of truth, this fitting procedure could be avoided if the chosen coordinates *really are* the reaction coordinates, but in practice, this situation never comes at hand if dealing with biological systems.

Results

In our numerical results, we have found that $I(V)$ characteristics are very sensitive to the values assumed by α_b 's in eq 8, which express the fraction of the total applied bias associated with each of the four steps reported in the previous section. Barriers used in our MC calculations range from 2.5 to 5.3 $k_B T$; higher values, as sometimes MD simulations provide, lead to current saturation at voltages much higher than those suggested by experiments. Furthermore, the existence of voltage-independent transition rates dominating the ion flow is suggested above 100 mV to account for current leveling-off, which in turn means that a dominating transition exists and somehow influences the conduction process at lower bias values.

We identify this crucial transition in the three-ion concerted motion $(S_1, S_3, S_{cav}) \leftrightarrow (S_0, S_2, S_4)$: it exhibits the highest barriers at zero bias, and it determines the order of magnitude of the current. To tune simulated data to experiments,⁹ we have found that most of the energy variation due to the external potential (about 90%) is affecting this transition (α_b

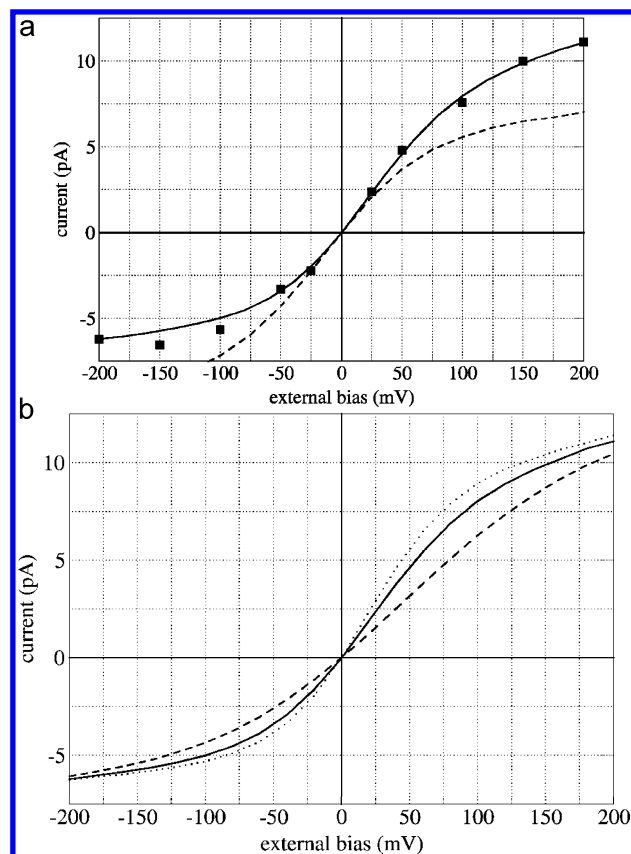


Figure 3. (a) Experimental and simulated $I(V)$ characteristics for K^+ ions flowing across the KcsA potassium channel (full squares refer to experiments⁹); the two curves refer to MC simulations obtained with a different distribution of the internal potential drop (dashed line mainly on the two-ion concerted motion, solid line mainly on the three-ion concerted motion). (b) Effect of the barrier height of the (t) transition on the current. The dashed and dotted lines represent calculations where $1 k_B T$ has been added to or subtracted from the original barrier height (solid line), respectively. A symmetric potassium concentration of 100 mM is used in all of the cases investigated. Positive bias is meant for a flux from the intracellular to the extracellular reservoir.

$= 0.9$), the residual energy being distributed $1/3$ to the transition to and from cavity S_{cav} ($\alpha_b = 0.033$) and $2/3$ to the transition from and to the outer mouth S_0 ($\alpha_b = 0.067$). The two-ion motion's rate is substantially unaltered. A similar qualitative behavior can be obtained considering the two-ion motion as the crucial transition and leaving unaltered the three-ion's one, but results are less satisfactory, giving origin to a worse representation of experimental data (see also Figure 3). This framework appears to be consistent with the one reported in the literature,⁷ where the transmembrane potential drops mainly in the selectivity filter and approximately $1/10$ elsewhere. The resulting $I(V)$ characteristics for potassium atoms are reported in Figure 3a together with available experimental results.⁹

To investigate how the results reported in Figure 3a are sensible to the values assumed by the barrier heights, we performed two simulations adding or subtracting $1 k_B T$ to the previously determined height of the (t) transition, which is supposed to mostly affect the permeation process, keeping

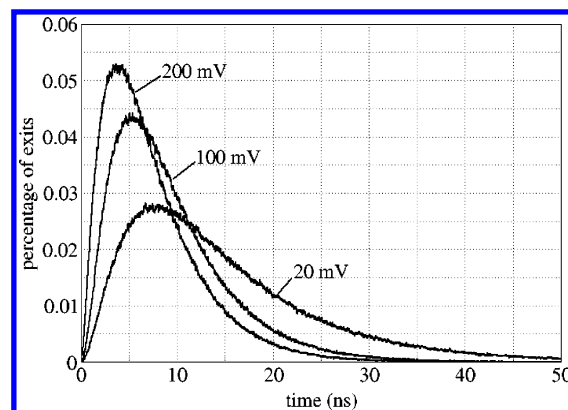


Figure 4. Number of ion exits as a function of the time interval between two successive ion exits from the simulation. Mean time and most frequent time are 14 ns and 7.8 ns at 20 mV, 9.3 ns and 5.3 ns at 100 mV, and 7.4 ns and 4.1 ns at 200 mV, respectively.

the prefactor A in eq 8 fixed. This value is approximately the minimum standard deviation associated with the estimates from MD simulations. Results are shown in Figure 3b. It is seen that the three curves in the figure are qualitatively similar and converge to values close to each other at the highest (positive or negative) fields. This is so because the electrostatic energy contribution coming from the external bias gains more importance in the determination of the exponent in eq 8 under the above-mentioned conditions. Moreover, the considered barrier is significantly lowered by the effect of the field, and the barriers associated with other transitions still play an important role, as discussed above. On the contrary, at low and intermediate biases, the difference in the conductance for the three cases is relevant, and the agreement with experiments is lost, especially when the barrier height is increased. It should be observed, however, that the prefactor and the exponent in eq 8 are equally important in the determination of the numerical value of the rate itself.

From the computational point of view, shot noise can be analyzed even at frequencies corresponding to the characteristic microscopic time of single shots, provided that the current sampling time is properly chosen. To estimate this characteristic time for the process under investigation, we have evaluated the number of ion exits as a function of the time interval elapsed since the previous exits. The obtained distribution exhibits a maximum, and the length of its tail depends on the external bias, as shown in Figure 4. For a bias of 100 mV, the peak of the curve is obtained at a time of 5.3 ns, while the average time $\langle T_{\text{exit}} \rangle$ between two successive ion exits is estimated approximately as 9.3 ns.

Figure 5 shows the power spectrum of current fluctuations normalized to $2q\langle I \rangle$ as a function of frequency from simulations which use different values of the current sampling time Δt . It can be noted that the low- and high-frequency ranges are not affected by the choice of Δt . On the contrary, at frequencies on the order of $1/\langle T_{\text{exit}} \rangle$, the shape of the spectrum strongly depends on the choice of Δt , as it should happen also in experimental measurements, because of the limitations imposed in the frequency range of the Fourier transform.

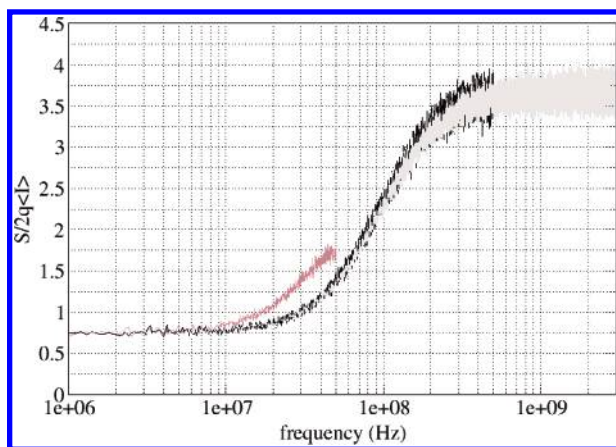


Figure 5. Power spectrum of the current fluctuations as a function of frequency as obtained from the simulations using different sampling times for the current signal. The dark line is obtained with a sampling time of $\Delta t = 10^{-9}$ s, the half-tone gray line with a sampling time of $\Delta t = 10^{-8}$ s, and the pale gray line with a sampling time of $\Delta t = 10^{-10}$ s. The three results have been obtained at the same bias of 100 mV.

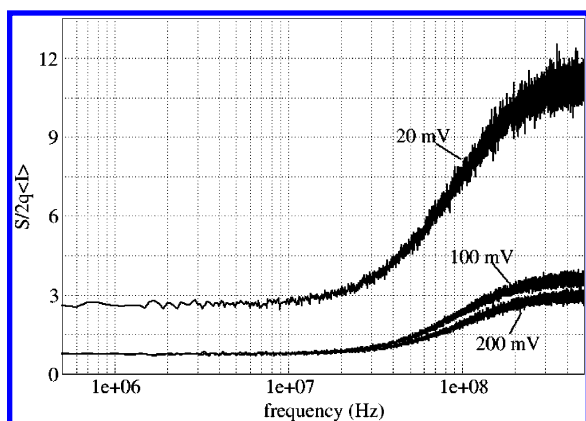


Figure 6. Power spectrum of the current fluctuations as a function of frequency obtained with different values of the external bias, indicated in the figure. All of the results refer to the same potassium concentration of 100 mM.

Examples of calculated noise power spectra as functions of frequency at different external biases are shown in Figure 6.

White noise is found until about 2×10^7 Hz; at frequencies on the order of $1/\langle T_{\text{exit}} \rangle$, an increase of the spectrum is observed, up to the highest considered frequencies, where single charge output is seen.

The asymptotic value of $S_I(\omega)$ in the low-frequency range can be exploited to calculate the system conductance G without application of any transmembrane potential by means of the Nyquist formula:²⁹

$$S_I(\omega) = 4k_B T \operatorname{Re}[1/Z(\omega)] \quad (9)$$

where $Z(\omega)$ is the system impedance. In the considered low-frequency range, the dispersion can be neglected, and $1/Z(\omega) \cong G$. Equation 9 can be reformulated as follows:

$$G = S_I(0)/4k_B T \quad (10)$$

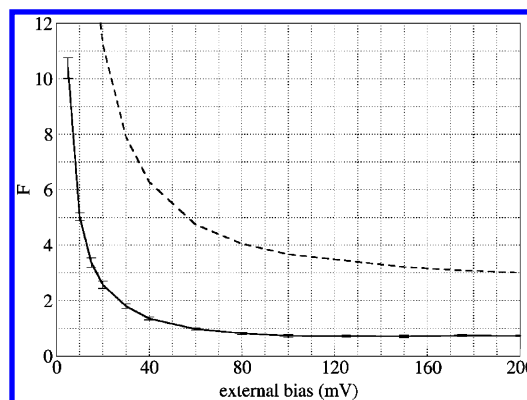


Figure 7. Fano factor as a function of the external bias for the power spectrum shown in Figure 5. The dashed line refers to a process with two totally uncorrelated opposite currents, as from eq 5 (see text).

$S_I(0)$ being the limit of $S_I(\omega)$ in the low-frequency region. For this purpose, the average value in the range 50–500 kHz was considered (lower frequencies do not introduce significant differences in the evaluation of the average). For the zero-bias condition, we obtain a conductance $G = 91 \pm 2$ pS; the corresponding value that can be inferred from experimental data reported in Figure 3 is 96 pS. The agreement between these two data further confirms the consistency of the calculations.

Finally, in Figure 7 the Fano factor obtained from eq 4 is plotted as a function of the external bias. The same result is obtained from both positive and negative biases, and for this reason, negative biases are not reported in the figure. F rapidly decreases at increasing bias until about 100 mV, where an asymptotic value of 0.73 is reached. To estimate the effect of correlations in the ions' motion on the noise spectrum, we reported in the same figure the Fano factor F^* calculated from the MC simulation with eq 5, assuming that the two opposite currents (with net flux equal to I) are totally uncorrelated.

The two curves are qualitatively similar, and their ratio ranges from a factor 4 to a factor 5 over the range of the considered biases. The comparison between F and F^* allows us to state that the increase of the Fano factor at low biases is mainly because of the numbers of ions' crossings in the two directions tend to become equal, and exits immediately followed by a re-entrance are very frequent. The presence of a significant external bias imposes the dominance of one of the two fluxes over the other. Moreover, the numerical differences between F and F^* confirm the existence of a significant correlation in the ions' motion due to the peculiar permeation paths affecting the conduction process.

Conclusions

A numerical procedure for the evaluation of the conduction and noise associated with ion flow across membrane channels has been presented. The occupancy configurations of the channel, the transition rates between different configurations, and the parameters contained in the transition-rate formula have been evaluated through MD simulations and from a comparison with experimental data. Numerical results obtained from a MC procedure for the case of potassium ions

permeating the KcsA channel provide $I(V)$ characteristics comparable with experimental data, once the drop of the external field is accurately modeled. The current noise power spectrum exhibits a structure suggesting significant correlation between successive ion exits. This computational analysis shows that noise measurements in single open channels, today achievable with modern equipment, can contribute to the comprehension of the permeation mechanisms inside the channel.

Acknowledgment. We thank A. Bigiani, J. Kona, C. Miller, M. Rosini, and F. Sigworth for useful discussions.

References

- (1) Traynelis, S. F.; Jaramillo, F. Getting the Most out of Noise in the Central Nervous System. *TINS* **1998**, *21*, 137–145.
- (2) Miller, C. Private communication.
- (3) Heinemann, S. H.; Sigworth, F. J. Open Channel Noise. V. Fluctuating Barriers to Ion Entry in Gramicidin A Channels. *Biophys. J.* **1990**, *57*, 499–514.
- (4) Krasilnikov, O. V.; Bezrukov, S. M. Polymer Partitioning from Nonideal Solutions into Protein Voids. *Macromolecules* **2004**, *37*, 2650–2657.
- (5) Zhou, Y.; Morais-Cabral, J.; Kaufman, K.; MacKinnon, R. Chemistry of Ion Coordination and Hydration Revealed by a K⁺ Channel–Fab Complex at 2.0 Å. *Nature* **2001b**, *414*, 43–48.
- (6) Roux, B.; Allen T.; Bernèche S.; Im W. Theoretical and Computational Models of Biological Ion Channels. *Q. Rev. Biophys.* **2004**, *37*, 15–103.
- (7) Bernèche, S.; Roux, B. A Microscopic View of Ion Conduction through the K⁺ Channel. *Proc. Natl. Acad. Sci. U.S.A.* **2003**, *100*, 8644–8648.
- (8) Kutluay, E.; Roux, B.; Heginbotham, L. Rapid Intracellular TEA Block of the KcsA Potassium Channel. *Biophys. J.* **2005**, *68*, 1018–1029.
- (9) LeMasurier, M.; Heginbotham, L.; Miller, C. KcsA: It's a Potassium Channel. *J. Gen. Physiol.* **2001**, *118*, 303–313.
- (10) Morais-Cabral, J.; Zhou, J. H.; MacKinnon, R. Energetic Optimization of Ion Conduction Rate by the K⁺ Selectivity Filter. *Nature* **2001**, *414*, 37–42.
- (11) Compain, M.; Carloni, P.; Ramseyer, C.; Girardet, C. Molecular Dynamics Study of the KcsA Channel at 2.0-Å Resolution: Stability and Concerted Motions within the Pore. *Biochim. Biophys. Acta* **2004**, *1661*, 26–39.
- (12) Roux, B. Ion Conduction and Selectivity in K⁺ Channels. *Annu. Rev. Biophys. Biomol. Struct.* **2005**, *34*, 153–171.
- (13) Souaille, M.; Roux, B. Extension to the Weighted Histogram Analysis Method: Combining Umbrella Sampling with Free Energy Calculations. *Comput. Phys. Commun.* **2001**, *35*, 40–57.
- (14) Hummer, G.; Szabo, A. Free Energy Reconstruction from Nonequilibrium Single-Molecule Pulling Experiments. *Proc. Natl. Acad. Sci. U.S.A.* **2001**, *98*, 3658–3661.
- (15) Hummer, G.; Szabo, A. Free Energy Surfaces from Single-Molecule Force Spectroscopy. *Acc. Chem. Res.* **2005**, *38*, 504–513.
- (16) Laio, A.; Parrinello, M. Escaping Free Energy Minima. *Proc. Natl. Acad. Sci. U.S.A.* **2002**, *99*, 12562–12566.
- (17) Piccinini, E.; Ceccarelli, M.; Affinito, F.; Brunetti, R.; Jacoboni, C. Exploring Free-Energy Profiles through Ion Channels: Comparison on a Test Case. *J. Comput. Electron.* **2006**, to be published.
- (18) Hanggi, P.; Talkner, P.; Borkovec, M. Reaction-Rate Theory: Fifty Years after Kramers. *Rev. Mod. Phys.* **1990**, *62*, 251–341.
- (19) Siwy, Z.; Ausloos, M.; Ivanova, K. Correlation Studies of Open and Closed State Fluctuations in an Ion Channel: Analysis of Ion Current through a Large-Conductance Locust Potassium Channel. *Phys. Rev. E: Stat. Phys., Plasmas, Fluids, Relat. Interdiscip. Top.* **2002**, *65*, 0319071–0319075.
- (20) Frehland, E.; Stephan, W. Theory of Single-File Noise. *Biochim. Biophys. Acta* **1979**, *553*, 326–341.
- (21) Schottky, W. Über Spontane Stromschwankungen in Verschiedenen Elektrizitätsleitern. *Ann. Phys. (Leipzig)* **1917**, *57*, 541–567.
- (22) Fano, U. Ionization Yield of Radiation. II. The Fluctuations of the Number of Ions. *Phys. Rev.* **1947**, *72*, 26–29.
- (23) Lindhal, E.; Hess, B.; van der Spoel, D. GROMACS 3.0: A Package for Molecular Simulation and Trajectory Analysis. *J. Mol. Model.* **2001**, *7*, 306–317.
- (24) Berendsen, H. J. C.; van der Spoel, D.; van Drunen, R. GROMACS: A Message-Passing Parallel Molecular Dynamics Implementation. *Comput. Phys. Commun.* **1995**, *91*, 43–56.
- (25) Essman, U.; Perela, L.; Berkowitz, M. L.; Darden, T.; Lee, H.; Pedersen, L. G. A Smooth Particle Mesh Ewald Method. *J. Chem. Phys.* **1995**, *103*, 8577–8592.
- (26) Kumar, S.; Bouzida, D.; Swedesen, R. H.; Kollman, P. A.; Rosenberg, J. M. The Weighted Histogram Analysis Method for Free-Energy Calculations on Biomolecules. I. The Method. *J. Comput. Chem.* **1992**, *13*, 1011–1021.
- (27) Yeh, I.; Berkowitz, M. L. Dielectric Constant of Water at High Electric Fields: Molecular Dynamics Study. *J. Chem. Phys.* **1999**, *110*, 7935–7942.
- (28) Yeh, I.; Hummer, G. Nucleic Acid Transport through Carbon Nanotube Membranes. *Proc. Natl. Acad. Sci. U.S.A.* **2004**, *101*, 12177–12182.
- (29) Nyquist, H. Thermal Agitation of Electric Charge in Conductors. *Phys. Rev.* **1928**, *32*, 110–113.

CT6002077